Lawrence Berkeley Laboratory
UNIVERSITY OF CALIFORNIA

ENERGY & ENVIRONMENT DIVISION

Presented at the Annual Meeting of the American Society of Civil Engineers, New Orleans, LA, October 23-29, 1982

WIND AND INFILTRATION INTERACTION FOR SMALL BUILDINGS

M.H. Sherman and D.T. Grimsrud

October 1982

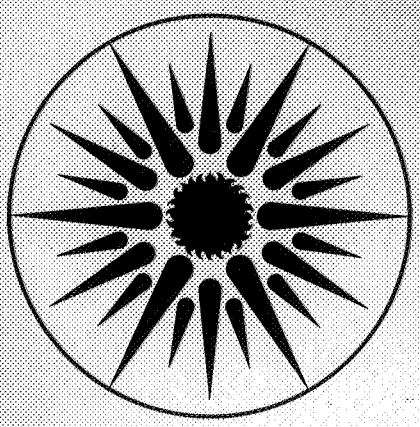

ENERGY AND ENVIRONMENT DIVISION

Prepared for the U.S. Department of Energy under Contract DE-AC03-76SF00098

LBL-13949
EEB-epb-82-5

Contribution to the Annual Meeting of the American Society of Civil Engineers, New Orleans LA, October 23-29, 1982.

WIND AND INFILTRATION INTERACTION FOR SMALL BUILDINGS

M. H. Sherman and D. T. Grimsrud

Energy Performance of Buildings Group
Lawrence Berkeley Laboratory
University of California
Berkeley Ca 94720

Wind is one of the key environmental variables that drives energy loss processes in small (residential-scale) buildings. The major influence of the wind is observed in infiltration, the random leakage of outside air into the conditioned volume of a building. A model, developed by the authors, that predicts infiltration from both wind and temperature influence to within 20% will be presented. A comparison is made between the predicted and the measured infiltration from a full-scale test structure, revealing an average discrepancy of less than 10 m^3/hr (out of an average of approximately 150 m^3/hr). Direct measurements of the wind velocity and pressure coefficients induced by the wind on the full-scale test structure are also presented.

This work was supported by the Assistant Secretary for Conservation and Renewable Energy, Office of Building Energy Research and Development, Building Systems Division of the U.S. Department of Energy under Contract No. DE-AC03-76SF00098.

MOBILE INFILTRATION TEST UNIT (MITU)

MITU[1] was built using a commercially available construction-site office trailer that was modified and instrumented by researchers at LBL. Illustrated in Figure 1, MITU is a portable, self-contained test structure designed to perform extended infiltration field studies in a variety of climates, allowing complete control of building and site parameters. It is instrumented to assist with validation of both long-term average and hour-by-hour infiltration-model predictions. The trailer is also designed to test various components of the model individually: it translates airport wind data into wind at the structure, reduces wind-induced pressures due to localized shielding, etc.

MITU is a wood-frame structure, 4.9 m (16 ft) long, 2.4 m (8 ft) wide, and 2.4 m (8 ft) high. It contains both heating and cooling systems and requires only electrical power at a site. The walls and floor of the trailer contain a total of sixteen window openings that can be fitted with interchangeable calibrated leakage panels for controlling total leakage, leakage distribution, and leakage type (such as narrow cracks or large holes). The trailer shell is sealed with a continuous vapor barrier, and perforations are caulked with silicone sealant to minimize leakage. The leakage of the panels and the trailer shell are determined with a specially designed fan pressurization system that fits into one of the window openings and uses an orifice plate to measure air flow. Air infiltration, weather data, and surface pressures are sampled, reduced, and recorded on floppy disks by a Z-80 based microprocessor.

Air Infiltration

Air infiltration is monitored with the Continuous Infiltration Monitoring System (CIMS) developed at LBL.[2] This system computes and stores half-hour average infiltration rates.

This work was supported by the Assistant Secretary for Conservation and Renewable Energy, Office of Building Energy Research and Development, Building Systems Division of the U.S. Department of Energy under Contract No. DE-AC03-76SF00098.

Wind Speed and Wind Direction

Wind speed and wind direction are measured at two heights, 5.5 m (18 ft) and 10 m (33 ft) above the ground. The sensors are mounted on collapsible weather towers that are permanently affixed to the rear of the trailer. Outdoor temperature is monitored by a sensor mounted 7 m (23 ft) above the ground. Speeds, directions, and temperatures are checked every minute and recorded on disk as half-hour averages.

Surface Pressures

Surface pressures from 82 taps located on the walls, floor, and ceiling are measured with differential pressure transducers. Taps are opened and closed by computer-controlled solenoid valves. During sampling, each tap is kept open for two seconds. The pressures are monitored with pressure transducers on six levels: four of the transducers are on the walls at 0.23m (0.75 ft), 0.90m (2.95 ft), 1.57m (5.15 ft), and 2.24m (7.35 ft) above the floor of the trailer, while the remaining two transducers are on the ceiling and floor. All pressures, including inside pressure (measured with an additional transducer), are measured relative to the static pressure in the wind. This system allows direct measurement of stack-induced pressures and the height of the neutral level. The zero of each transducer is checked every half-hour and subtracted from the surface pressures, which are then stored as thirty-minute averages.

The static pressure in the wind is measured using a static pressure probe which was designed, built, and calibrated by David Wilson of the Mechanical Engineering Department of the University of Alberta in Edmonton, Canada. The probe is relatively insensitive to horizontal wind direction, having a pressure coefficient of 0.07. It is also insensitive to the vertical component of the wind within ten degrees of the horizontal. Using the static pressure in wind allows us to measure the external (and internal) pressure coefficients as well as the outside-inside pressure differences.

INFILTRATION MODEL

The residential infiltration model developed at LBL[3-5] uses the concept of effective leakage area along with building and site parameters to make infiltration predictions from available weather data. The model was specifically designed for simplicity; precise detail was sacrificed for ease of application. The functional form of the model, along with some important assumptions, is presented below:

$$Q = L \sqrt{f_s^2 \Delta T + f_w^2 v^2} \qquad (1)$$

where

- Q is the infiltration [m^3/s],
- L is the effective leakage area [m^2],
- ΔT is the indoor-outdoor temperature difference [K],
- f_s is the stack parameter [$m/s/K^{1/2}$],
- v is the wind speed, and
- f_w is the wind parameter.

In this expression f_w and f_s, the wind and stack parameters, convert the wind speed v and the indoor-outdoor temperature difference ΔT into equivalent pressures across the leakage area of the house, as defined in the references. (The terms inside the square root have units of velocity squared, that is, pressure over density.) The wind and stack parameters are weather-independent, depending upon the distribution of leakage area, the degree to which the house is shielded from the wind, and building height. Typical values for the stack and wind parameters for an average single-story, single-family dwelling are given below:

$$f_s = 0.120 \quad \frac{m}{s} K^{-1/2} \qquad (2.1)$$

$$f_w = 0.123 \qquad (2.2)$$

For buildings that are more (less) exposed to the wind, the wind parameter may increase (decrease) by as much as 50%. In the same way, a structure with large vertical distance between leaks in the envelope will have a large stack parameter.

Before expressions for terms f_s and f_w can be given, two additional quantities must first be introduced; the fraction of the total leakage

in the floor and ceiling divided by the total, R:

$$R = \frac{L_c + L_f}{L} \tag{3}$$

The fractional difference between the ceiling leakage area L_c, and floor leakage area L_f is called X.

$$X = \frac{L_c - L_f}{L} \tag{4}$$

The stack parameter is expressed in these terms as well as by the acceleration of gravity g [9.8 m/s^2] and the absolute indoor temperature T [295 K]:

$$f_s = \frac{1}{3}(1 + \frac{R}{2}) \left[1 - \frac{X^2}{(2 - R)^2}\right]^{3/2} \left[\frac{gH_s}{T}\right]^{1/2} \tag{5}$$

where

R is the vertical leakage fraction,

X is the ceiling/floor leakage difference,

H_s is the height from the lowest to highest leakage site [m].

The wind parameter is also expressed in these quantities but further includes the shielding coefficient C' (see Table 1) and the terrain parameters α and γ (see Table 2):

$$f_w = C' (1 - R)^{1/3} \left[\frac{\alpha_h (H_w/10)^{\gamma_h}}{\alpha_m (H_m/10)^{\gamma_m}}\right] \tag{6}$$

where

C' is the shielding coefficient for the house site,

R is the fractional horizontal leakage area,

α_h, γ_h are terrain constants for the house,

H_w is the height from grade to the top of the living space [m],

α_m, γ_m are terrain constants for the wind measurement site, and

H_m is the height of the wind measurement site [m].

Because in most buildings the lowest leak is near grade level and the highest leak is near the ceiling, we can assume that the stack height and wind height are equal:

$$H_s \simeq H_w \tag{7}$$

Although there are special cases in which the distinction between stack height and wind height is important, we generally ignore it and use the definition of wind height as the operational definition of the height of the structure.

The wind pressures on the surface of a building depend upon both the terrain class and the shielding class of the structure. Most airport wind-speed measurements are made in terrain class II, while most houses are located in terrain classes III or IV. The values of α and γ for standard terrain classes are presented in Table 1 below.[6]

Table 1: **Terrain parameters for standard terrain classes.**

Class	γ	α	Description
I	0.10	1.30	Ocean or other body of water with at least 5 km of unrestricted expanse.
II	0.15	1.00	Flat terrain with some isolated obstacles (e.g. buildings or trees well separated from each other).
III	0.20	0.85	Rural areas with low buildings, trees, etc.
IV	0.25	0.67	Urban, industrial, or forest areas.
V	0.35	0.47	Center of large city (e.g. Manhattan).

Terrain effects are primarily large-scale effects caused by the roughness of the boundary layer in the region surrounding the structure; they determine the (height) profile of the wind. To find the wind speed at the site, the meteorological wind speed is corrected using both the terrain classes of the site and the weather station:

$$v_o = v \frac{\alpha_h (H_w/10)^{\gamma_h}}{\alpha_m (H_m/10)^{\gamma_m}} \qquad (8)$$

where

v_o is the local wind speed [m/s].

Shielding and Pressure Coefficients

While terrain effects primarily concern widespread effects on the boundary layer, shielding is a local phenomenon. Shielding produces mitigation of wind pressure by obstructions in the immediate surroundings of the building, such as foliage, fences, or other buildings. In this sense the generalized shielding coefficient, which is a macroscopic property of the entire building, is very closely related to the external pressure coefficients, which relate the pressure rise on the face of the building to the dynamic pressure of the wind:

$$C_j = \frac{P_j}{1/2\,\rho v_o^2} \qquad (9)$$

where

C_j is the pressure coefficient on the jth face,
P_j is the rise in static pressure on the jth face [Pa], and
ρ is the density of air [1.2 kg/m^3].

There is also an inside pressure coefficient C_o, which relates the change in interior pressure to the wind speed; it is defined as above.

We can use pressure coefficients to calculate the wind driven infiltration. The flow through each crack will be proportional to the square root of the pressure across it, which will be proportional to the pressure coefficient. Because there will be both infiltration and exfiltration, which should balance, we estimate the total flow by taking an average of the infiltration and exfiltration summed over each face of the structure:

$$Q_{wind} = \frac{v_o}{2} \sum_j L_j \sqrt{|C_j - C_o|} \qquad (10)$$

where

Q_{wind} is the wind pressure induced infiltration [m^3/s] and
L_j is the leakage area of the jth site [m^2].

If we compare this expression to the wind-generated part of our infiltration expression we find the following relation:

$$L\, C' \,(\, 1 - R \,)^{1/3} = 1/2 \sum_j L_j \sqrt{\left| C_j - C_o \right|} \qquad (11)$$

For the special case of the leakage area being evenly distributed around the walls, we can solve for the generalized shielding coefficient:

$$C' = 1/2 \left[\sqrt{\left| C_j - C_o \right|} \right] \qquad (12)$$

where

$\left[\ldots \right]$ indicates a spatial average.

This equation and boundary-layer wind-tunnel data for an isolated structure[7] were used to calculate the shielding coefficient. This value corresponds to our least shielded case; other cases were calculated as fractions of the least shielded case. The values of the generalized shielding coefficients C' for the five classes are presented in Table 2 below.

The least shielded case, shielding class I, corresponds to a building isolated from any obstructions that might affect the wind pressures. The most shielded case, shielding class V, corresponds to a highly congested area with almost no direct wind exposure; the pressures on the building are dominated by turbulence. Our experience has shown that urban areas most typically have class IV shielding; suburban areas generally have class III shielding; and rural areas usually have class II shielding.

MEASURED DATA

Although MITU has been on station in Reno, Nevada, for the winters of 1980-1981 and 1981-1982, we concentrate our attention on a ten-day period in late March and early April, 1982. The wind during the period from March 27 through March 29 and April 2 through April 5th was quite strong and reasonably steady, affording good measurements of the pressure coefficients and other wind-induced effects. MITU was positioned so that its long axis was aligned with north. (The long axis is 16 ft; the

Table 2: **Generalized shielding coefficient vs. local shielding.**

Shielding Class	C'	Description
I	0.324	No obstructions or local shielding whatsoever (i.e. isolated building).
II	0.285	Light local shielding with few obstructions (e.g. a few trees or a shed in the vicinity).
III	0.240	Moderate local shielding; some obstructions within two house heights (e.g. thick hedge or fence and nearby buildings).
IV	0.185	Heavy shielding; obstructions around most of perimeter buildings or trees within five building-heights in most directions (e.g. well-developed/dense tract houses).
V	0.102	Very heavy shielding, large obstruction surrounding perimeter within two house heights (e.g. typical downtown area).

short axis 8 ft.)

Figures 2 and 3 show the distribution of wind speed and direction during these two periods. Figure 4 is a polar plot of the wind speed vs. wind direction. These three figures show all of the wind measurements made during the test period.

Pressure coefficients were measured simultaneously and individually for each pressure tap and averaged for each half-hour period. Figures 5 through 9 show the distribution of measured pressure coefficients as a function of incident wind direction, averaged for the four faces of MITU, and the internal pressure. For the pressure coefficients, all points having a wind speed less than 3.5 m/s were deleted from the data; this removed points outside of the -60° to $+120^{\circ}$ cone. These points were removed because stack-induced pressures make measurement of the pressure coefficient inaccurate for low wind speeds.

As presented above, our model can predict the infiltration from the wind speed and temperature data. Figure 10 compares our predicted infiltration with the infiltration measured by the tracer-gas system for a two-day period beginning March 27th. Gaps in the measured curve

indicate periods when the measurement system was not functional.

DISCUSSION

From the wind speed and direction profiles we see that for the test period the wind is rather evenly distributed in the 5 to 10 m/s and -60° to 120° ranges. From the velocity profile we see that the majority of high-speed points cluster in the -45° to 0° range.

Although the generalized shielding coefficients were not calculated, measurement of pressure coefficients will yield some understanding of the shielding around the MITU trailer. The south-face pressures follow expected behavior: the pressure coefficient approaches a minimum of about -1 at an angle near 0°, and then increases smoothly from there. The east and west faces show similar behavior for the non-windward faces (i.e. $< 0^{\circ}$ for the east face and $> 0^{\circ}$ for the west face), but the windward faces that should have large positive ($\simeq 1$) coefficients, have coefficients much closer to zero. This behavior is typified by the north-face pressures, which hover near zero at angles from -45° to 45° and even become negative very close to a due north wind.

We believe this result is due to the obstruction of the north face of MITU by the air-conditioner, tracer-gas supply, and trailer hitch assemblies, which induce extra turbulence and deflect the wind around the north face, causing some suction pressures. This hypothesis is supported by the internal pressure coefficient, which -- especially near due north -- exhibits behavior very similar to the north face. If the north face pressure is close to the internal pressure, there will be no net flow through the north face, as would be the case if the surface pressure were highly turbulent.

Because of the interference of the north-face equipment and the unidirectionality of the wind, we did not collect the type of data we had hoped for. In the future, however, we expect to make more pressure measurements using MITU and full-scale buildings to understand the spatial and directional behavior of pressure coefficients. We also expect to use pressure measurements to calculate the generalized shielding coefficients directly; this ability will enable us to use wind-tunnel

data for estimating infiltration.

REFERENCES

1. Blomsterberg, A. K., Modera, M.P., and Grimsrud, D.T. 1981. The Mobile Infiltration Test Unit-- Its Design and Capabilities: Preliminary Experimental Results. Lawrence Berkeley Laboratory Report, LBL 12259.

2. Sherman, M. H., Grimsrud, D. T., Condon, P. E., and Smith, B. V. 1980. Air Infiltration Measurement Techniques. Proc. of the 1st AIC Conf., London.
Lawrence Berkeley Laboratory Report, LBL 10705.

3. Sherman, M.H. 1980. Air Infiltration in Buildings. Ph.D. thesis, University of California.
Lawrence Berkeley Laboratory Report, LBL 10712.

4. Sherman, M.H., Grimsrud, D.T. 1980, The Measurement of Infiltration Using Fan Pressurization and Weather Data. Proc. of 1st AIC Conf., London.
Lawrence Berkeley Laboratory Report, LBL 10852.

5. Sherman, M.H., Sonderegger, R.C., and Grimsrud, D.T. The LBL Infiltration Model. Unpublished.

6. European Convention for Constructional Steelwork. 1978. Recommendations for the Calculation of Wind Effects on Buildings and Structures. Technical General Secretariat, Brussels, Belgium.

7. Akins, R.E, Peterka, J.A., and Cermak, J.E. 1979. Average Pressure Coefficients for Rectangular Buildings. Proceedings of the Fifth Int. Conf. Wind Engineering, Boulder, Colorado.

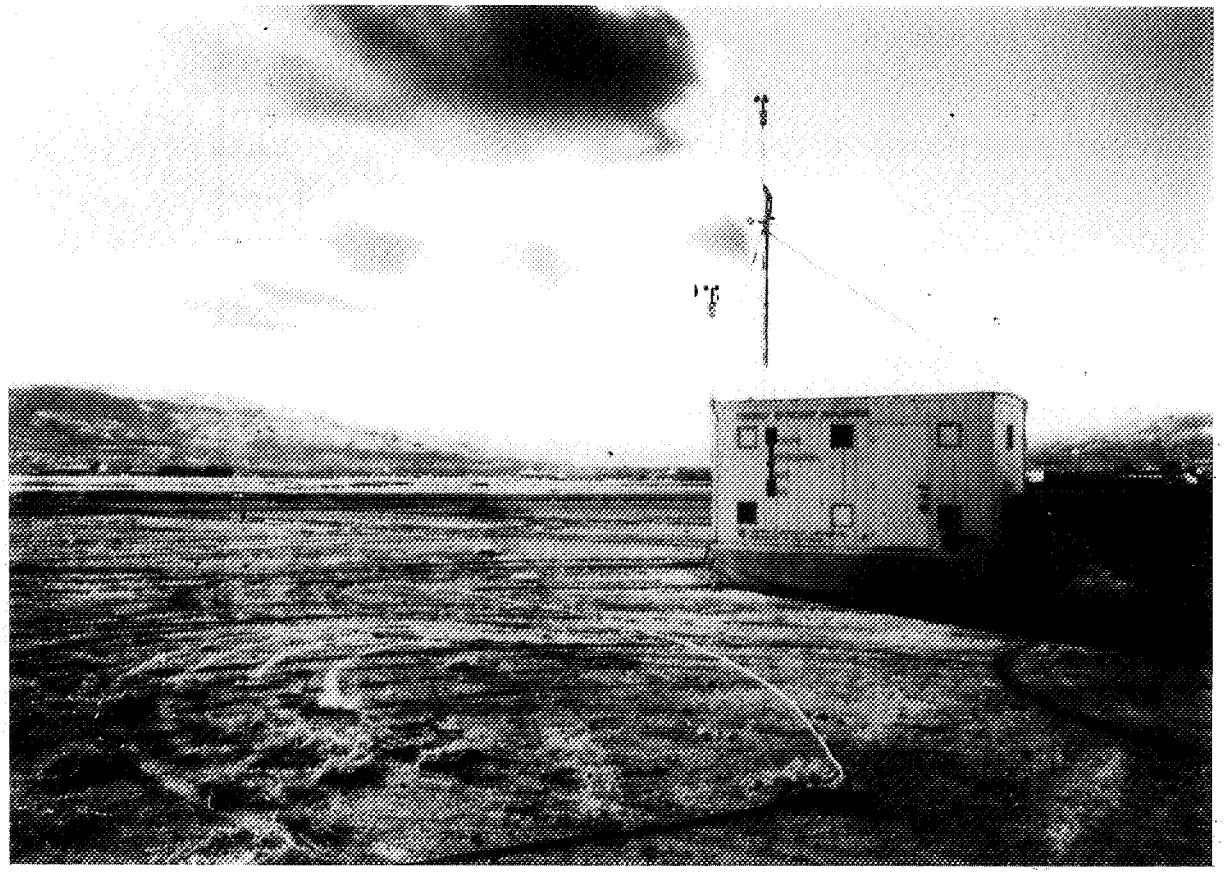

CBB 828-7302

Figure 1. Mobile Infiltration Test Unit on site in Reno, Nevada.

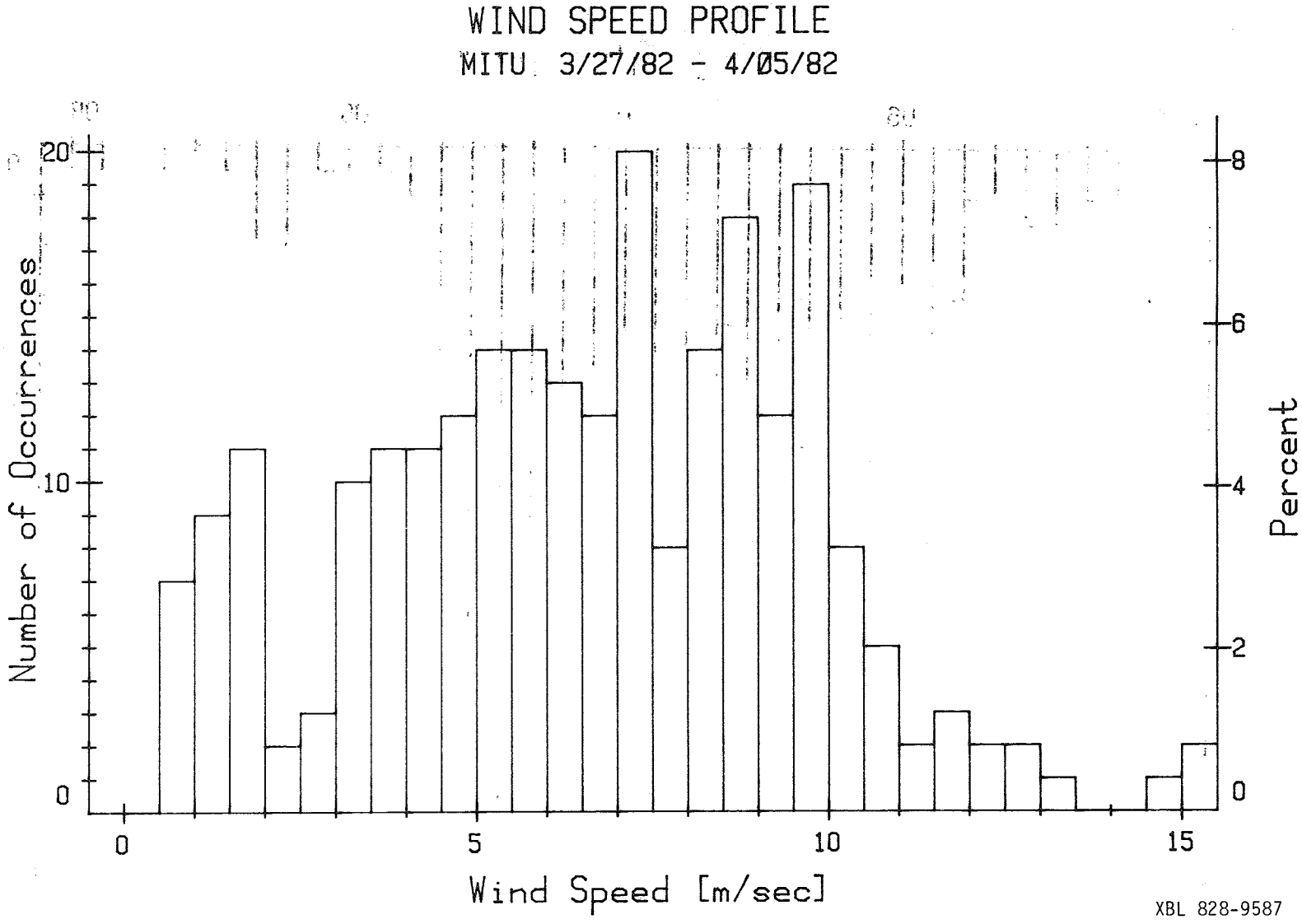

Figure 2. Histogram of the wind speed during the test period.

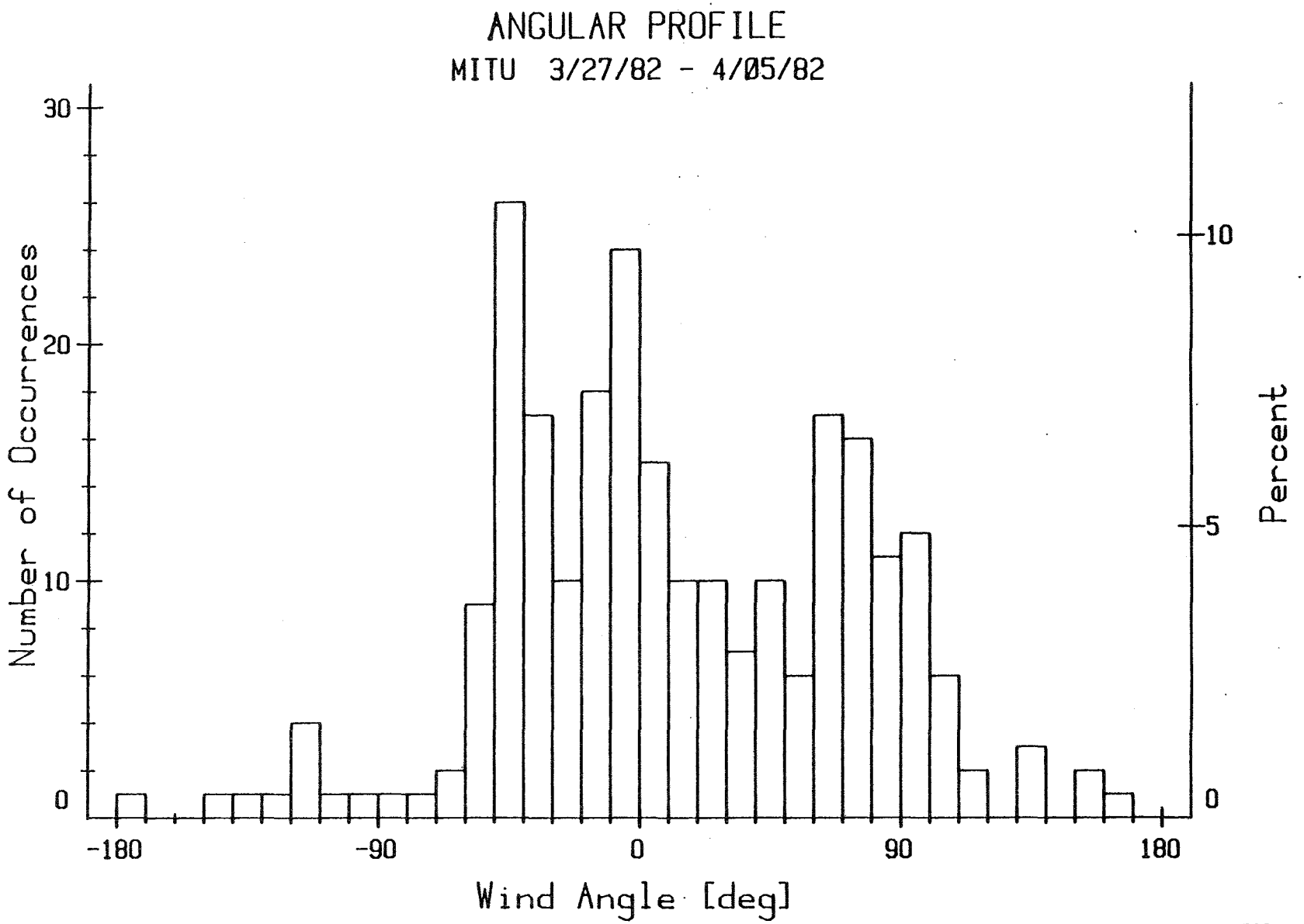

Figure 3. Histogram of the wind direction during the test.

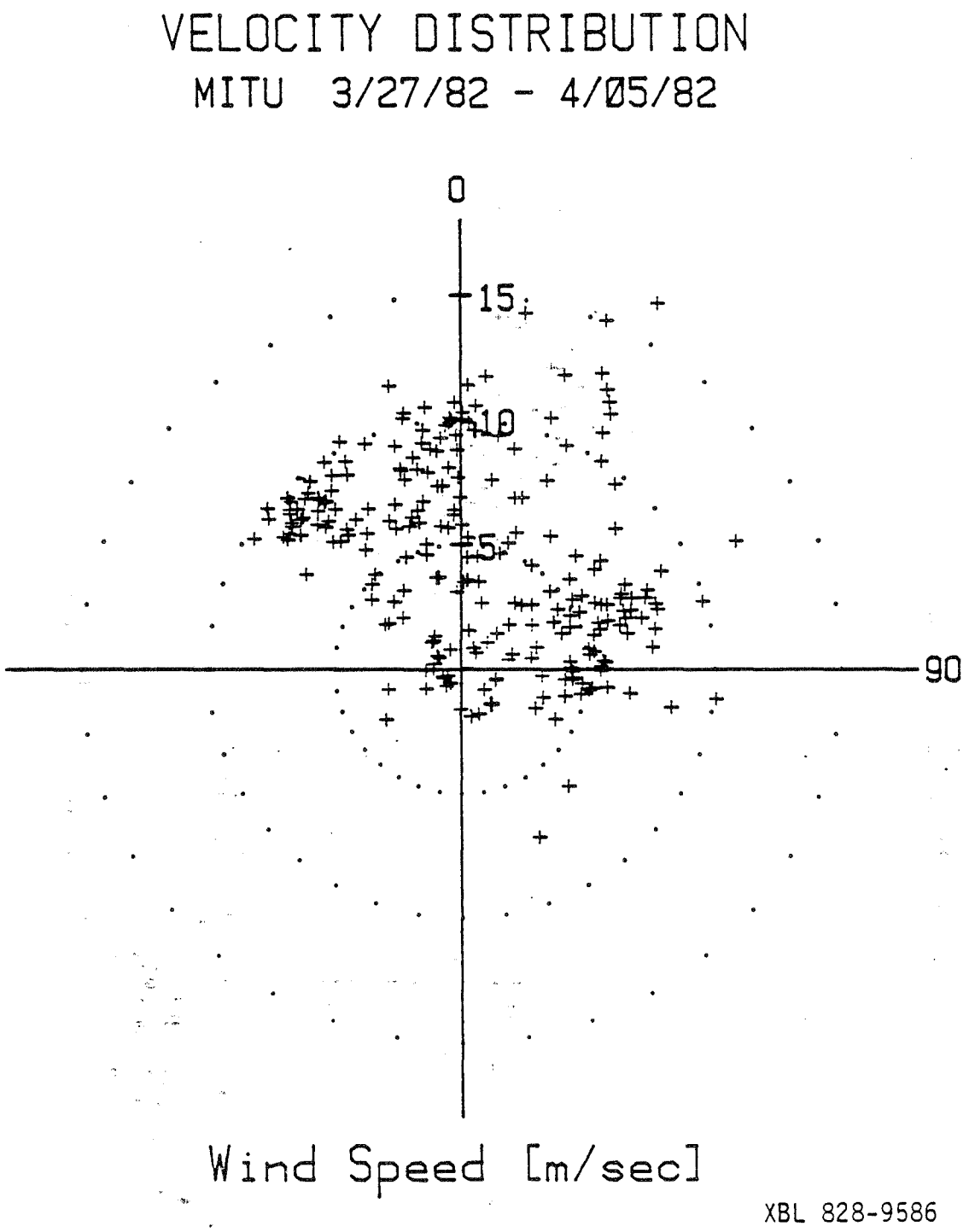

Figure 4. Polar plot of the wind speed vs. wind direction during the test.

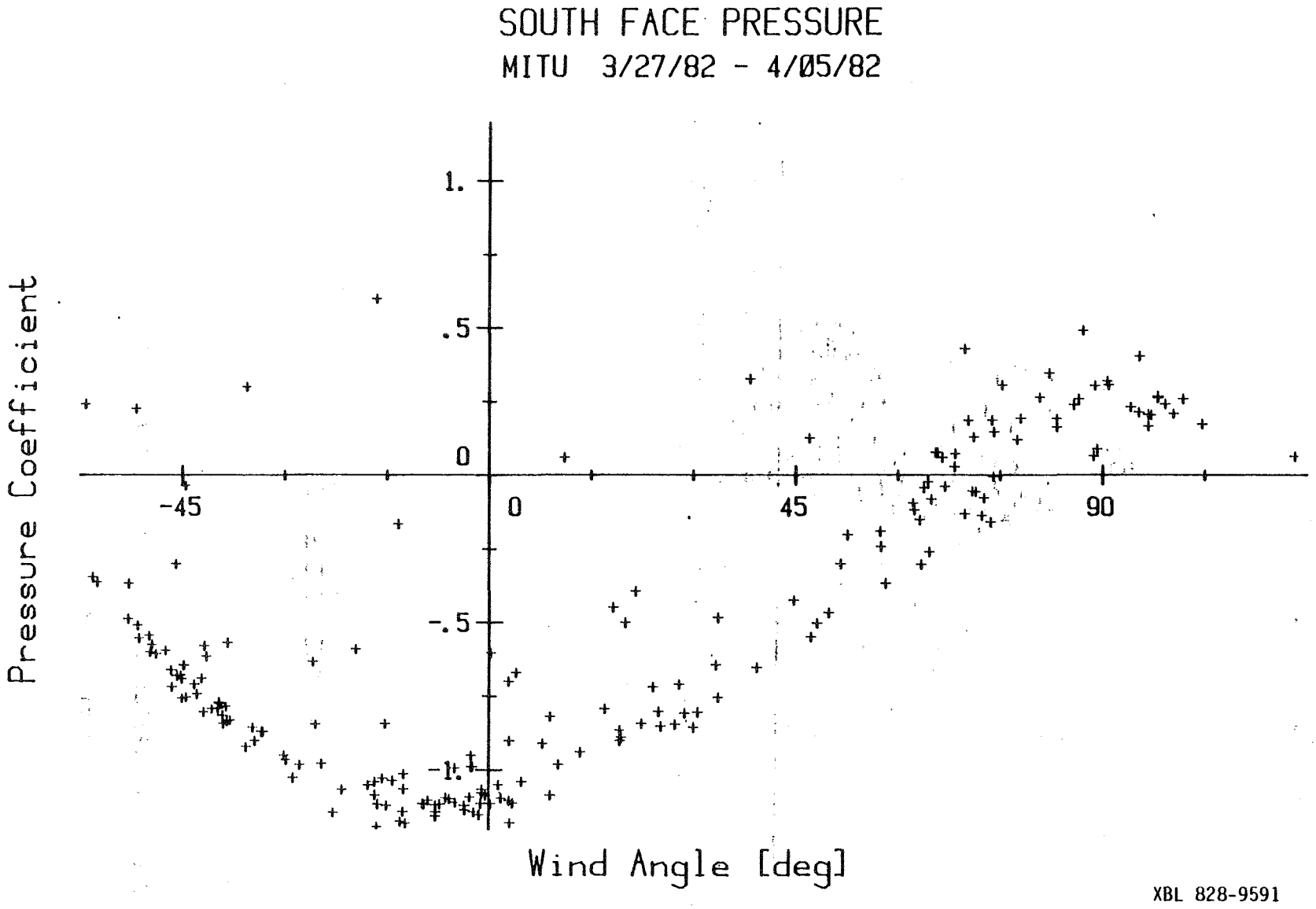

Figure 5. Plot of half-hour shielding coefficients for the south face.

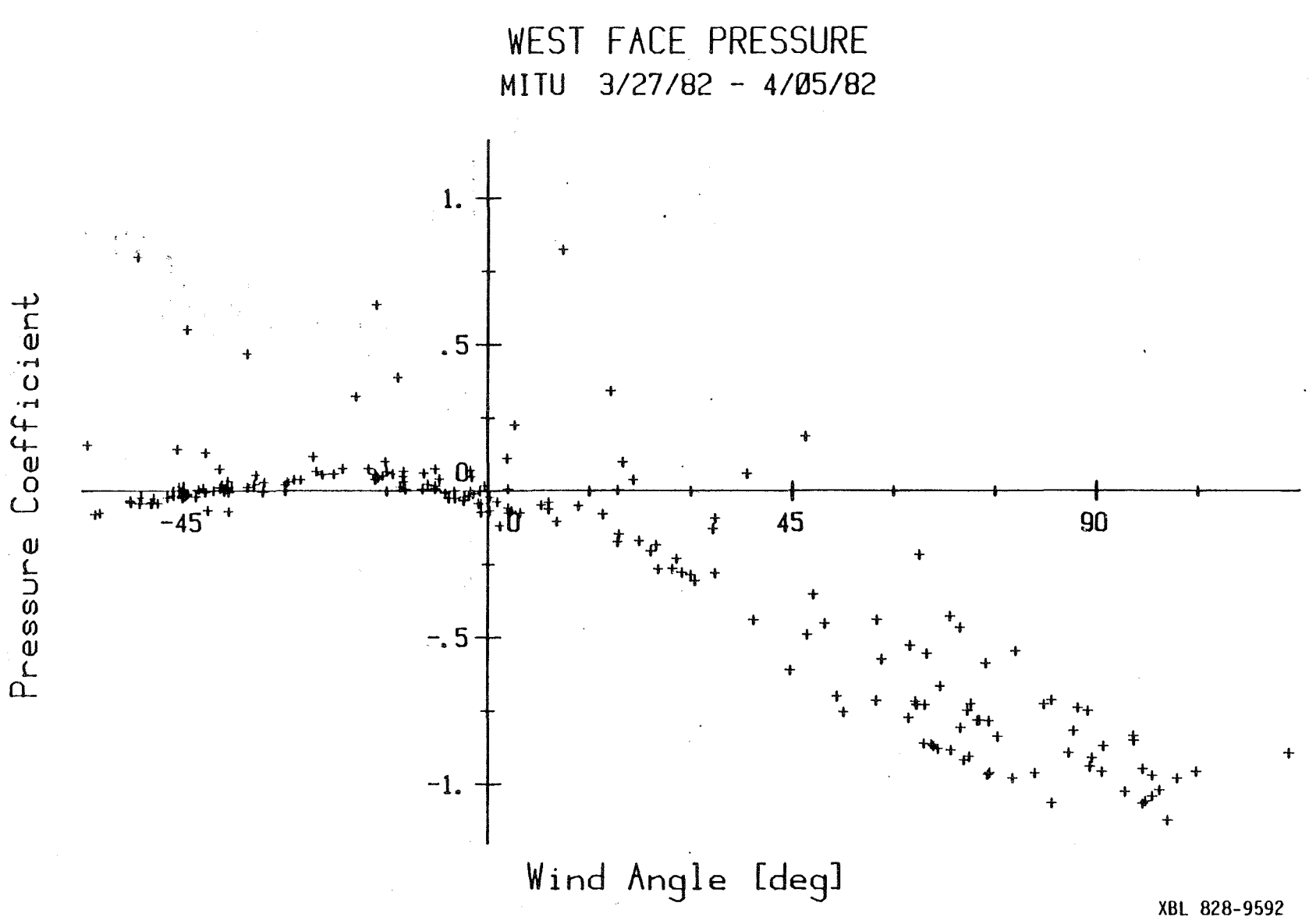

Figure 6. Plot of half-hour shielding coefficients for the west face.

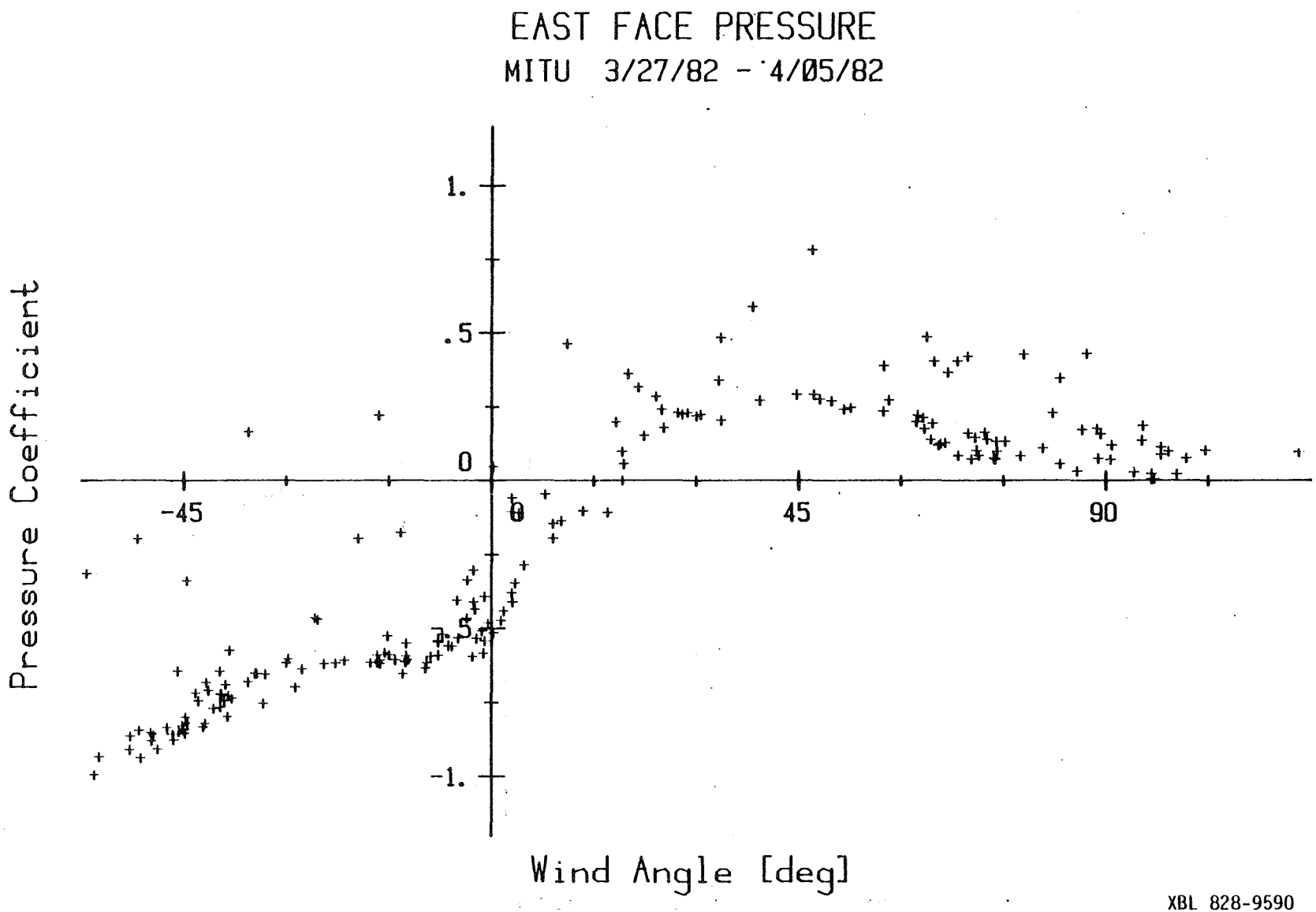

Figure 7. Plot of half-hour shielding coefficients for the east face.

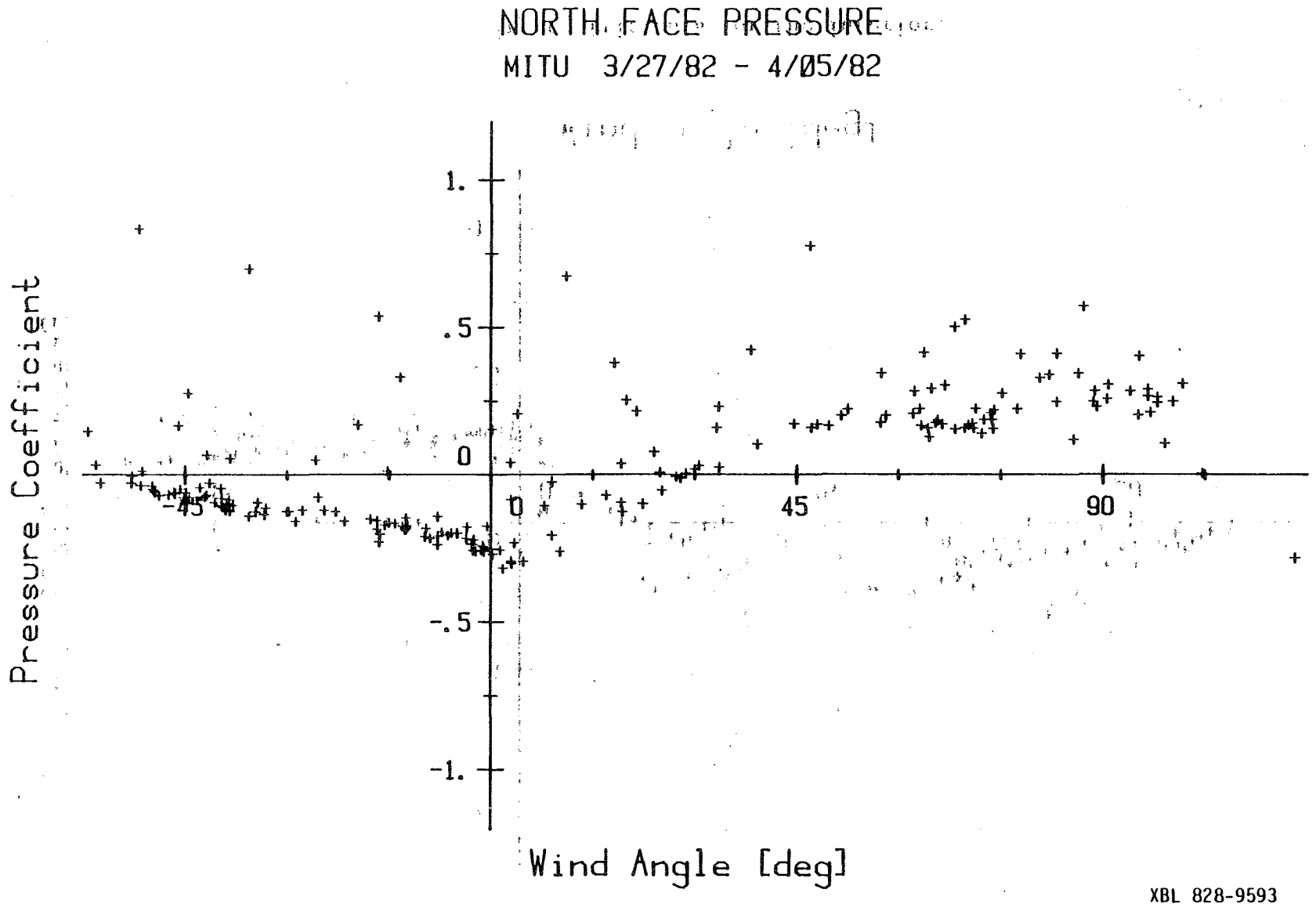

Figure 8. Plot of half-hour shielding coefficients for the north face.

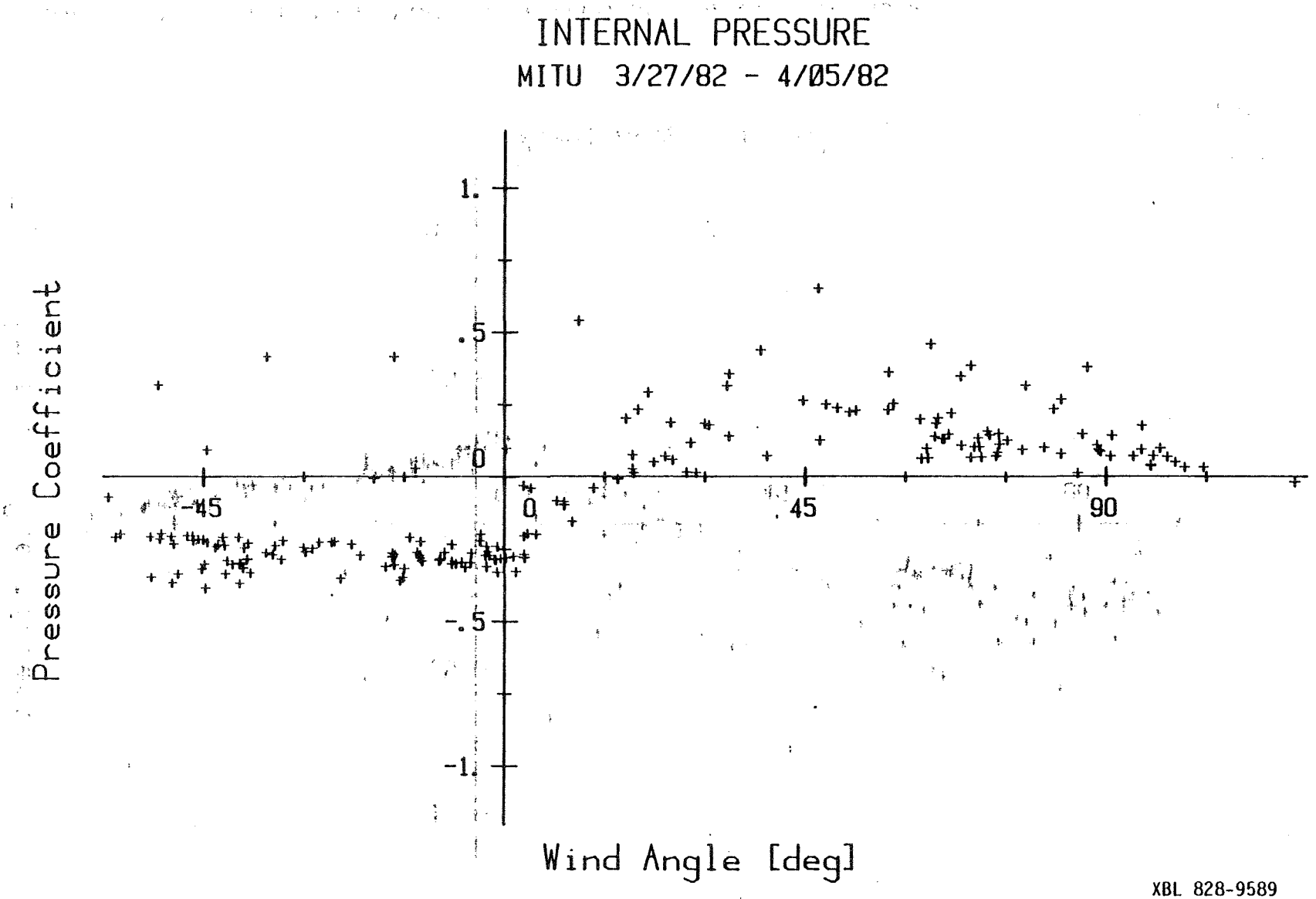

Figure 9. Plot of half-hour shielding coefficients for the interior.

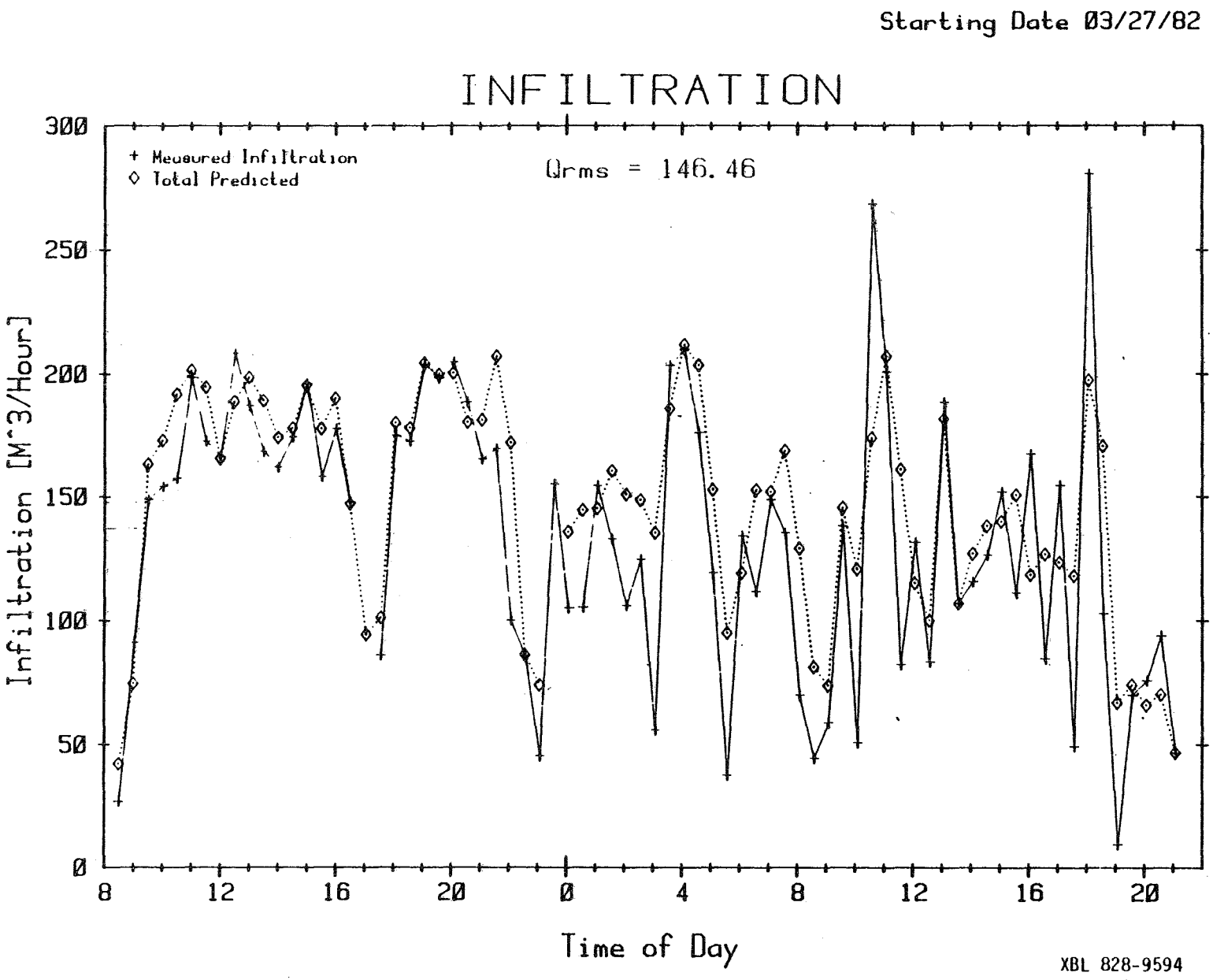

Figure 10. Measured and predicted infiltration during the test.